IJC
International Journal of Cancer

JAK–STAT signalling controls cancer stem cell properties including chemotherapy resistance in myxoid liposarcoma

Soheila Dolatabadi[1], Emma Jonasson[1], Malin Lindén[1], Bentolhoda Fereydouni[1], Karin Bäcksten[1], Malin Nilsson[2], Anna Martner[2], Amin Forootan[1,3], Henrik Fagman[1,4], Göran Landberg[1], Pierre Åman[1] and Anders Ståhlberg[1,4,5]

[1]Sahlgrenska Cancer Center, Department of Pathology and Genetics, Institute of Biomedicine, Sahlgrenska Academy at University of Gothenburg, Gothenburg, Sweden
[2]TIMM Laboratory, Sahlgrenska Cancer Center, University of Gothenburg, Gothenburg, Sweden
[3]MultiD Analysis AB, Gothenburg, Sweden
[4]Department of Clinical Pathology and Genetics, Sahlgrenska University Hospital, Gothenburg, Sweden
[5]Wallenberg Centre for Molecular and Translational Medicine, University of Gothenburg, Gothenburg, Sweden

Myxoid liposarcoma (MLS) shows extensive intratumoural heterogeneity with distinct subpopulations of tumour cells. Despite improved survival of MLS patients, existing therapies have shortcomings as they fail to target all tumour cells. The nature of chemotherapy-resistant cells in MLS remains unknown. Here, we show that MLS cell lines contained subpopulations of cells that can form spheres, efflux Hoechst dye and resist doxorubicin, all properties attributed to cancer stem cells (CSCs). By single-cell gene expression, western blot, phospho-kinase array, immunoprecipitation, immunohistochemistry, flow cytometry and microarray analysis we showed that a subset of MLS cells expressed JAK–STAT genes with active signalling. JAK1/2 inhibition *via* ruxolitinib decreased, while stimulation with LIF increased, phosphorylation of STAT3 and the number of cells with CSC properties indicating that JAK–STAT signalling controlled the number of cells with CSC features. We also show that phosphorylated STAT3 interacted with the SWI/SNF complex. We conclude that MLS contains JAK–STAT-regulated subpopulations of cells with CSC features. Combined doxorubicin and ruxolitinib treatment targeted both proliferating cells as well as cells with CSC features, providing new means to circumvent chemotherapy resistance in treatment of MLS patients.

Molecular Cancer Biology

Introduction

The FET family of genes, *FUS*, *EWSR1* and *TAF15* (also known as *TLS*, *EWS* and *TAF12N*, respectively), are expressed in most tissues and cell types.[1] They encode homologous RNA-binding proteins involved at several levels of gene regulation.[2] More than 20 different sarcoma and leukemia entities are defined by fusion oncogenes with FET genes as 5′ partners and with alternative transcription-factor-coding genes as 3′ partners.[3,4] Myxoid liposarcoma (MLS) is the second most common type of liposarcoma and is characterized by the *FUS-DDIT3* or the less common *EWSR1-DDIT3* fusion oncogenes. Between 10 and 15% of the tumours contain subpopulations of round cells associated with increased cell density and more aggressive disease.[5] Most MLS tumours are genetically stable with functional TP53 system and few mutations in addition to the fusion oncogene.[6] A majority of MLS patients are successfully treated with a combination of surgery, radiotherapy and chemotherapy, but some cases remain a clinical problem.

Key words: cancer stem cells, chemotherapy resistance, JAK–STAT signalling, LIF, myxoid liposarcoma, ruxolitinib, SWI/SNF
Additional Supporting Information may be found in the online version of this article.
Grant sponsor: Barncancerfonden; **Grant number:** 2017-0043; **Grant sponsor:** Cancerfonden; **Grant numbers:** 2015-7130, 2016-438; **Grant sponsor:** Stiftelsen Assar Gabrielssons Fond; **Grant sponsor:** Svenska Sällskapet för Medicinsk Forskning; **Grant sponsor:** Vetenskapsrådet; **Grant number:** 2017-01392; **Grant sponsor:** Wilhelm and Martina Lundgren Foundation for Scientific Research; **Grant sponsor:** VINNOVA; **Grant sponsor:** The Swedish state under the agreement between the Swedish government and the county councils, the ALF-agreement; **Grant numbers:** 722211, 716321; **Grant sponsor:** Knut and Alice Wallenberg Foundation, Wallenberg Centre for molecular and translational medicine at University of Gothenburg, Sweden; **Grant sponsor:** Johan Jansson Foundation for Cancer Research; **Grant sponsor:** BioCARE National Strategic Research Program at University of Gothenburg
DOI: 10.1002/ijc.32123
This is an open access article under the terms of the Creative Commons Attribution-NonCommercial License, which permits use, distribution and reproduction in any medium, provided the original work is properly cited and is not used for commercial purposes.
History: Received 29 May 2018; Accepted 7 Jan 2019; Online 8 Jan 2019
Correspondence to: Anders Ståhlberg, Sahlgrenska Cancer Center, University of Gothenburg, Box 425, Gothenburg 405 30, Sweden, Tel.: +46 31 7866735; E-mail: anders.stahlberg@gu.se

10970215, 2019, 2, Downloaded from https://onlinelibrary.wiley.com/doi/10.1002/ijc.32123 by Statens Beredning, Wiley Online Library on [03/06/2023]. See the Terms and Conditions (https://onlinelibrary.wiley.com/terms-and-conditions) on Wiley Online Library for rules of use; OA articles are governed by the applicable Creative Commons License

What's new?

Despite improved survival of patients, existing therapies for Myxoid liposarcoma (MLS) present shortcomings as they fail to target all tumour cells. The nature of chemotherapy-resistant cells in MLS remains unknown, however. Here, the authors show that myxoid liposarcomas are heterogeneous and contain subpopulations of cells with stem cell properties, including chemotherapy resistance. Moreover, JAK-STAT signalling is active in MLS and regulates the size of the cancer stem cells-like subpopulation *via* the SWI/SNF complex. The results shed light on the mechanisms of therapy resistance in MLS and point to JAK-STAT inhibitors as a new avenue for targeted MLS therapies.

MLS is believed to originate from mesenchymal stem cells[3,7] and several studies have reported large intratumoural heterogeneity.[8,9] These observations suggest that MLS may contain distinct subpopulations of cells, including lipoblasts, senescent cells and proliferating progenitor cells.[10] Failures of modern cancer chemotherapies commonly depend on the survival of minorities of resistant tumour cells. The appearance of chemotherapy-resistant cells was until recently thought to be caused by new mutations leading to expression of multidrug resistance genes. This view has been challenged as normal adult tissue stem cells were reported to express drug resistance genes, a property also found in tumour cells with stem cell characteristics, i.e. cancer stem cells (CSCs).[11] Hence, a possible explanation for chemotherapy resistance in MLS is that certain tumour cells maintain some of their stem-cell-associated drug resistance features. However, existence, characteristics and functions of potential CSCs in MLS remain unknown.

The aim of this study was to search for and characterize cells with CSC properties in MLS. To assess the presence of cells with CSC features, we performed non-adherent sphere formation assay, Hoechst dye side population (SP) analysis and tested cells for chemotherapy resistance. The canonical JAK–STAT signalling pathway has been outlined in detail for several cell types, including CSCs, and various tumour entities,[12,13] but its role in MLS is mainly unknown. Here, we defined a role for JAK–STAT signalling by controlling the number of cells with CSC properties in MLS. Targeting chemotherapy-resistant cells with CSC properties with JAK–STAT inhibitors opens up new means for targeted MLS therapies.

Materials and Methods

Additional details are provided in Supporting Information and methods (see Supporting Information material).

Cell culture

The myxoid liposarcoma (MLS) cell lines 2645-94, 1765-92 and 402-91[14] were cultured in complete medium, containing RPMI 1640 GlutaMAX medium supplemented with 5% fetal bovine serum, 100 U/mL penicillin and 100 μg/mL streptomycin (all Thermo Fisher Scientific, Waltham, MA, USA), at 37°C in 5% CO_2. Cell passage was performed with 0.25% trypsin and 0.5 mM EDTA (Thermo Fisher Scientific). Cells ($2\text{-}3 \times 10^5$) were seeded in 6-well plates (TPP, Trasadingen, Switzerland) and cultured for 24 h before treatment with ruxolitinib (Selleckchem, Munich, Germany), leukemia inhibitory factor (LIF) (Merck, Darmstadt, Germany) doxorubicin (Sigma-Aldrich, St. Louis, MO, USA) or SMARCA4 RNAi (9634811, Invitrogen, CA, USA). Cells were treated for 24 h with 2.5 μM ruxolitinib or 30 ng/mL LIF, unless stated otherwise. In addition, all LIF experiments were performed using 1% fetal bovine serum. For doxorubicin experiments, cells were treated for 48 h using 140 nM, 120 nM and 30 nM for MLS 2645-94, 1765-92 and 402-91, respectively, unless stated otherwise. For combined ruxolitinib and doxorubicin treatments, MLS 2645-94 cells were pre-treated for 48 h, while MLS 1765-92 and 402-91 cells were pre-treated for 24 h. For SMARCA4 knock-down cells were transfected with either 20 nM SMARCA4 RNAi or 20 nM siRNA control (4390843, Thermo Fisher Scientific) for 48 h using HiPerFect transfection reagent according to the manufacturer's instructions (Qiagen, Hilden, Germany).

Non-adherent sphere formation assay

To enrich for cells with CSC properties, single-cell suspensions were seeded in 6-well plates (Eppendorf, Hamburg, Germany) pre-coated with 1.2% poly(2-hydroxyethyl methacrylate (Sigma-Aldrich) dissolved in 95% ethanol. For initial determination of sarcosphere formation efficiency, cells were seeded at a density of 2,000 cells per well in sphere medium containing phenol red-free DMEM/F-12, 2% B27 supplement (Thermo Fisher Scientific), 20 ng/mL epidermal growth factor (BD Biosciences, San Jose, CA, USA), 100 U/mL penicillin and 100 μg/mL streptomycin, as previously described.[15] The number of sarcospheres was counted after 72 h. For each experiment, three independent wells were calculated and averaged. Based on sarcosphere formation capacity, 500 (MLS 2645-94), 500 (MLS 1765-92) and 2,000 (MLS 402-91) cells per well were used for all additional non-adherent sphere formation assays. To test the effect of ruxolitinib, LIF, doxorubicin and SMARCA4 knock-down, cells were pre-treated in regular cell cultures before the non-adherent sphere forming assay.

Side population analysis

To analyse the side population, we applied the Hoechst staining method described by Goodell *et al.*[16] with minor modifications. Cells (10^6 cells/mL) were suspended in complete RPMI 1640 GlutaMAX medium and stained with Hoechst 34580 (Thermo Fisher Scientific) with a final concentration of 10 μg/mL and incubated in a shaking water-bath at 37°C for 60 min. Next,

cells were centrifuged at 85 rcf for 3 min, resuspended in complete medium and incubated at 37°C for additional 30 min, followed by centrifugation at 85 rcf for 3 min and resuspension in 2 mL ice cold Hanks' balanced salt solution (Thermo Fisher Scientific). Thereafter, 1 mg/mL propidium iodide (Sigma-Aldrich) was added to the cells at room temperature for 5 min. Cells were washed twice using 2 mL Hanks' balanced salt solution and kept in 1 mL Hanks' balanced salt solution. Cell aggregates were removed by filtering using a 70 μm cell strainer (BD Biosciences) and analyzed with a BD FACSAria II (BD Biosciences). To discriminate the side population cells from the main population, the ABC-transporters were inhibited using 50 μM verapamil hydrochloride (Sigma-Aldrich) as described.[17]

To test if anoikis-resistant cells contained elevated number of side population cells, 4×10^5 single MLS 2645-94 cells were seeded in sphere medium in T175 flasks pre-coated with 1.2% poly(2-hydroxyethyl methacrylate) dissolved in 95% ethanol. After 16 h incubation, cells were harvested by centrifugation at 10 rcf for 3 min. Supernatant was discarded until 4–5 ml of medium was left, and cells were centrifuged again at 120 rcf for 5 min and dispersed using 0.25% trypsin and 0.5 mM EDTA. A single-cell suspension was obtained using a 25 G needle and trypsin was inactivated with 4 mL fetal bovine serum. After a centrifugation at 580 rcf for 5 min, cells were resuspended in complete RPMI 1640 GlutaMAX medium and forwarded to side population assay.

Cell proliferation

Cell proliferation was analysed using Alamar Blue assay according to the manufacturer's instructions (Thermo Fisher Scientific). To determine IC_{50}-values, 1×10^4 cells per well were seeded into 96-well plates (TPP). Cells were treated 24 h after seeding with either 0.08–10 μM ruxolitinib for 72 h or 0.35–1,400 nM doxorubicin for 28 h. To assess cell proliferation, Alamar Blue was added to the cells and incubated for 3 h at 37°C. Fluorescence intensity was monitored in a VICTOR3 microplate reader (PerkinElmer, Waltham, MA, USA) using 540 nm excitation and 590 nm emission wavelengths. Wells containing medium and Alamar Blue without cells were used as control. The mean fluorescence of four replicate cultures was used for each time point and concentration. The IC_{50}-value was calculated from a dose response curve, using symmetrical sigmoidal curve fitting (GraphPad Prism 6.0, GraphPad Software, La Jolla, CA, USA).

Western blot

Cells for protein analysis were scraped in RIPA lysis buffer supplemented with 1x Halt Protease and Phosphatase Inhibitor Cocktail (both Thermo Fisher Scientific). Protein concentration was determined using DC protein assay (Bio-Rad, Hercules, CA, USA) according to the manufacturer's instructions. SDS-PAGE was performed with the NuPAGE system (Thermo Fisher Scientific), according to the manufacturer's instructions and transferred onto PVDF membranes (Thermo Fisher Scientific). Membranes were blocked with either 5% skim milk (Merck) or 5% bovine serum albumin (Sigma-Aldrich) in TBS-T buffer (50 mM Tris–HCl, pH 6.8, 50 mM NaCl, 0.05% Tween 20; all Sigma-Aldrich). Membranes were incubated overnight with primary antibodies against; JAK1 (#3332, Cell Signaling Technology, Danvers, MA, USA, diluted 1:1,000), JAK2 (#3230, Cell Signaling Technology, diluted 1:1,000), STAT3 (#12640, Cell Signaling Technology, diluted 1:1,000), phospho-STAT3 (#9131, Cell Signaling Technology, diluted 1:1,000), GAPDH (#ab9484, Abcam, Cambridge, UK, diluted 1:1,000). Detection was performed with Horseradish-Peroxidase-conjugated secondary antibodies (32430 or 32460, Thermo Fisher Scientific, diluted 1:1,000) combined with Supersignal West Dura Extended Duration Substrate (Thermo Fisher Scientific). Chemiluminescence was detected using ImageQuant LAS 4000 mini (GE Healthcare Life Sciences, Little Chalfont, UK) and bands were quantified using Multi Gauge (Fujifilm, Tokyo, Japan) or ImageJ.

Immunohistochemistry

Hematoxylin and eosin (H&E) staining was performed by standard methods using a Dako Autostainer system (Dako, Agilent, Santa Clara, CA, USA). Immunohistochemistry was performed on formalin-fixed, paraffin-embedded tumour resection specimens. In brief, antigen retrieval was performed in Dako PT-Link using EnVision™ FLEX Target Retrieval Solution (high pH). Immunohistochemical staining was performed in a Dako Autostainer Link using the EnVision™ FLEX detection system according to the manufacturer's instructions. Primary antibodies were anti phospo-STAT3 (ab76315, Abcam) and anti Ki67 (MIB1, Dako). Sections of lobular breast carcinoma were used as a positive control, showing nuclear positivity in normal ductal structures as well as in scattered tumour cell nuclei. Processing of patient material and data has been approved by the Regional Research Ethics Committee (REC) in Gothenburg (reference number: 133-11).

Single-cell gene expression analysis

MLS cells were dissociated with 0.25% trypsin and 0.5 mM EDTA, washed in PBS (pH 7.4, Thermo Fisher Scientific), resuspended in PBS supplemented with 2% bovine serum albumin (Sigma-Aldrich) and kept on ice until sorting. Cell aggregates were removed by filtering through a 70 μm cell strainer. Individual cells were sorted into 96-well PCR plates (Thermo Fisher Scientific), containing 5 μL 1 mg/mL bovine serum albumin and 2.5% glycerol (Thermo Fisher Scientific) using a BD FACSAria II. Sorted plates were immediately frozen on dry ice and stored at −80 °C.

Reverse transcription was performed using the GrandScript cDNA Synthesis Kit (TATAA Biocenter, Gothenburg, Sweden) on 5 μL cell lysate in a 10 μL reaction containing 1x TATAA GrandScript RT Reaction Mix and 1x TATAA GrandScript RT Enzyme. Reverse transcription was performed in a PTC-200 Thermal Cycler (MJ research, Bunker Lake

10970215, 2019, 2, Downloaded from https://onlinelibrary.wiley.com/doi/10.1002/ijc.32123 by Statens Beredning, Wiley Online Library on [05/05/2023]. See the Terms and Conditions (https://onlinelibrary.wiley.com/terms-and-conditions) on Wiley Online Library for rules of use; OA articles are governed by the applicable Creative Commons License

Blvd, Ramsey, MN, USA) at 25°C for 5 min, 42°C for 30 min and 85°C for 5 min.

Pre-amplification was performed using iQ Supermix (Bio-Rad) on 9 μL cDNA (diluted 1:4 in water) in a 30 μL reaction containing 1× iQ SYBR Green Supermix and a primer pool with 40 nM each of 150 primer pairs. Pre-amplification was run in a PTC-200 Thermal Cycler at 95°C for 3 min followed by 20 cycles of amplification at 95°C for 20 s, 55°C for 3 min and 72°C for 20 s followed by a final elongation step at 72°C for 10 min. Samples were frozen on dry ice.

Quantitative PCR was performed using SYBR GrandMaster Mix (TATAA Biocenter) on 1.5 μL pre-amplified cDNA (diluted 1:16 in TE buffer pH 8, Thermo Fisher Scientific), in a 6 μL reaction containing 1x SYBR GrandMaster Mix and 400 nM forward and reverse primers (Supporting Information Table S1). Quantitative PCR was run in a CFX384 Touch Real-Time PCR Detection System (Bio-Rad) at 95°C for 2 min followed by 50 cycles of amplification at 95°C for 5 s, 60°C for 20 s and 70°C for 20 s followed by melt curve analysis. Cycle of quantification values were determined by the second derivative maximum method using the CFX Manager Software version 3.1 (Bio-Rad). Single-cell data were pre-processed and analyzed as reported using the GenEx software (MultiD, Gothenburg, Sweden).[18] Briefly, a cycle of quantification cut-off value of 35 was applied and all values above were replaced with 35. Data were converted to relative quantities and missing data were replaced with 0.5 molecules. Heat-map analysis of Spearman's correlation coefficients was calculated using Ward's algorithm and Euclidean distance measure. Principle component analysis was performed on auto-scaled data.

Microarray analysis

MLS cell lines 2645-94, 1765-92 and 402-91 were treated with 45 nM of doxorubicin, applied every second day to the cells. Control cells together with treated cells were collected after 5 days. Total RNA was extracted using the RNeasy Micro Kit including DNase treatment (Qiagen) according to the manufacturer's recommendations and stored at −80°C. RNA quality was confirmed using Agilent RNA 6000 Nano Kit on a 2100 BioAnalyzer Instrument (Agilent) according to the manufacturer's recommendations.

For microarray analysis, 300 ng of total RNA was processed using the WT Expression Kit (Thermo Fisher Scientific) and 10 μg cRNA was obtained which was converted to ssDNA. Labelling and fragmentation was performed on 5.5 μg ssDNA using the GeneChipWT Terminal Labeling and Controls Kit (Thermo Fisher Scientific). Hybridization of 3.75 μg fragmented and labeled ssDNA, including hybridization controls, were performed using the GeneChip Human Gene 2.0 ST Array (Thermo Fisher Scientific) in 45°C for 16 h with 60 rpm rotation. Washing and staining of samples was performed using the GeneChip Hybridization Wash and Stain Kit on a GeneChip Fluidics Station 450 (both Thermo Fisher Scientific). Arrays were scanned using GeneChip Scanner 3000 7G with GeneChip Command Console software (both Thermo Fisher Scientific) and values were converted to log2-transformed, RMA-normalized values using the Expression Console Software (Thermo Fisher Scientific). Microarray data were obtained following the MIAME guidelines and are available at Gene Expression Omnibus with accession number GSE110997.

Expression values for all probes from doxorubicin-treated and control samples from cell lines 2645-94, 1765-92 and 402-91 were used. Probes with low average expression were filtered away using a cut-off of 3, leaving 50,293 probes left for analysis. Fold change values were calculated and probes at least two-fold regulated between treated and untreated cells for each cell line were selected. The probe set ID:s were converted to official gene symbols using the DAVID database. The numbers of regulated genes were calculated from the gene names obtained after this conversion. Genes upregulated in the doxorubicin-treated group in all three cell lines were matched against the Hallmark gene sets on the molecular signatures database (MSigDB) in order to identify functions and signalling pathways related to these genes. All gene sets with a false discovery rate (FDR)-adjusted q-value below 0.05 were included as significant.

Results

Identification of subpopulations with CSC characteristics in MLS

The ability of cells to form spheres under non-adherent conditions is a feature associated with CSCs.[19] Our data showed that the three tested MLS cell lines contained cells that were able to form non-adherent spheres (sarcospheres) with an efficiency of 22, 10 and 4% for MLS 2645-94, 1765-92 and 402-91, respectively (Fig. 1*a*). Next, we quantified the number of SP cells in MLS cell lines. In SP analysis, the ability of cells to efflux the Hoechst dye *via* the ATP-Binding Cassette (ABC) transporters is analyzed, where increased ABC transporter activity is an activity associated with CSCs.[19] MLS 2645-94, 1765-92 and 402-91 contained 0.8, 0.7 and 0.0% SP cells, respectively (Fig. 1*b*). To confirm the gating of SP cells, we treated cells with the ABC-transporter inhibitor verapamil. The number of SP cells was effectively decreased in verapamil-treated MLS 2645-94 and 1765-92 cells, validating the applied gating strategy to discriminate SP cells. To determine if the subpopulations of cells that form sarcospheres and efflux Hoechst dye are overlapping, we analyzed the number of SP cells in combination with anoikis resistance. Anoikis-resistant cells refer to cells surviving non-adherent conditions, harvested before forming spheres. Figure 1*c* shows that anoikis-resistant MLS 2645-94 cells generated higher number of SP cells compared to control cells.

Doxorubicin enriches for cells with CSC properties

Another feature of CSCs is resistance to chemotherapy.[20] We determined the IC_{50}-value of doxorubicin, a drug used as chemotherapy in MLS patients,[21] using Alamar Blue cell viability assay. The IC_{50}-values were 320, 110 and 29 nM for MLS

10970215, 2019, 2, Downloaded from https://onlinelibrary.wiley.com/doi/10.1002/ijc.32123 by Statens Beredning, Wiley Online Library on [03/06/2023]. See the Terms and Conditions (https://onlinelibrary.wiley.com/terms-and-conditions) on Wiley Online Library for rules of use; OA articles are governed by the applicable Creative Commons License

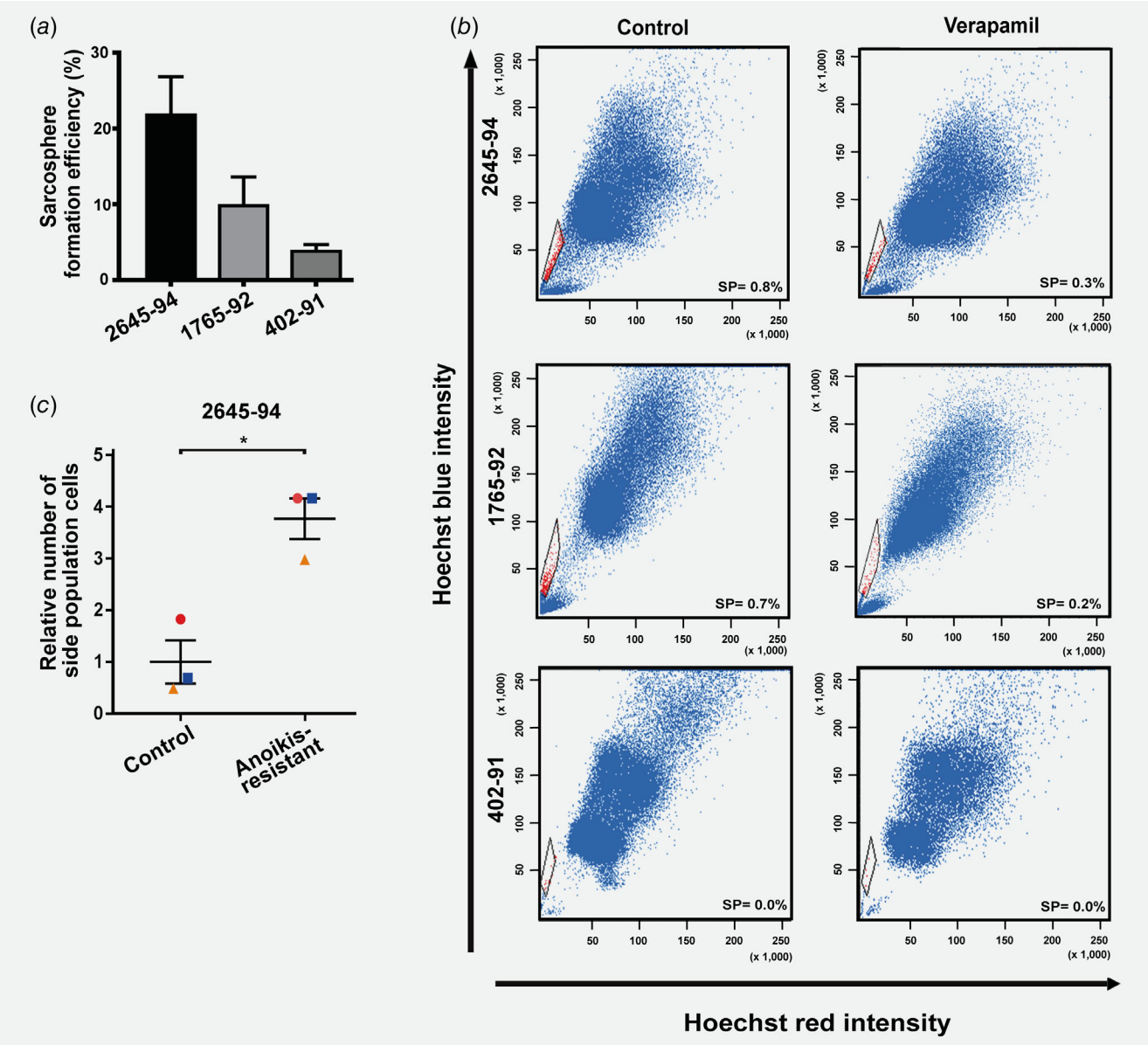

Figure 1. Sarcosphere formation and side population analysis in MLS. (*a*) Sarcosphere formation efficiency of MLS 2645-94, 1765-92 and 402-91 cells. The sarcosphere formation efficiency is calculated as the fraction of formed spheres in relation to the total number of seeded cells. Mean ± SEM is shown, n = 3. (*b*) Side population (SP) analysis of MLS 2645-94, 1765-92 and 402-91 using Hoechst dye staining. The left panel represents untreated control cells, while the right panel represents cells treated with verapamil. The SP cells (red) are gated and their fraction is compared to the total viable cell population. (*c*) SP analysis of anoikis-resistant cells compared to non-enriched control cells. Three independent experiments (red, orange and blue) were performed. Mean ± SEM is shown, paired student *t*-test $*p < 0.05$. [Color figure can be viewed at wileyonlinelibrary.com]

2645-94, 1765-92 and 402-91, respectively (Fig. 2*a*). To test whether doxorubicin treatment affects the number of CSCs, we performed both non-adherent sphere formation assay and SP analysis on doxorubicin pre-treated cells. Doxorubicin treatment resulted in 32, 180 and 39% more sarcospheres compared to control for MLS 2645-94, 1765-92 and 402-91, respectively (Fig. 2*b*). The SP analysis revealed 380, 210 and 43% more Hoechst-effluxing cells in the doxorubicin resistant population (Fig. 2*c*). In addition to the SP data we showed that the protein expression of ABCG2, a well-characterized ABC transporter,[22] was upregulated in doxorubicin-treated cells (Supporting Information Fig. S1). Altogether, these data show that doxorubicin treatment enriches for cells with CSC characteristics.

JAK–STAT signalling is active in MLS and controls CSC properties

JAK–STAT is known to regulate stem-cell related functions in cancer.[23,24] Binding of cytokine ligands to their associated

10970215, 2019, 2, Downloaded from https://onlinelibrary.wiley.com/doi/10.1002/ijc.32123 by Statens Beredning, Wiley Online Library on [05/02/2023]. See the Terms and Conditions (https://onlinelibrary.wiley.com/terms-and-conditions) on Wiley Online Library for rules of use; OA articles are governed by the applicable Creative Commons License

Molecular Cancer Biology

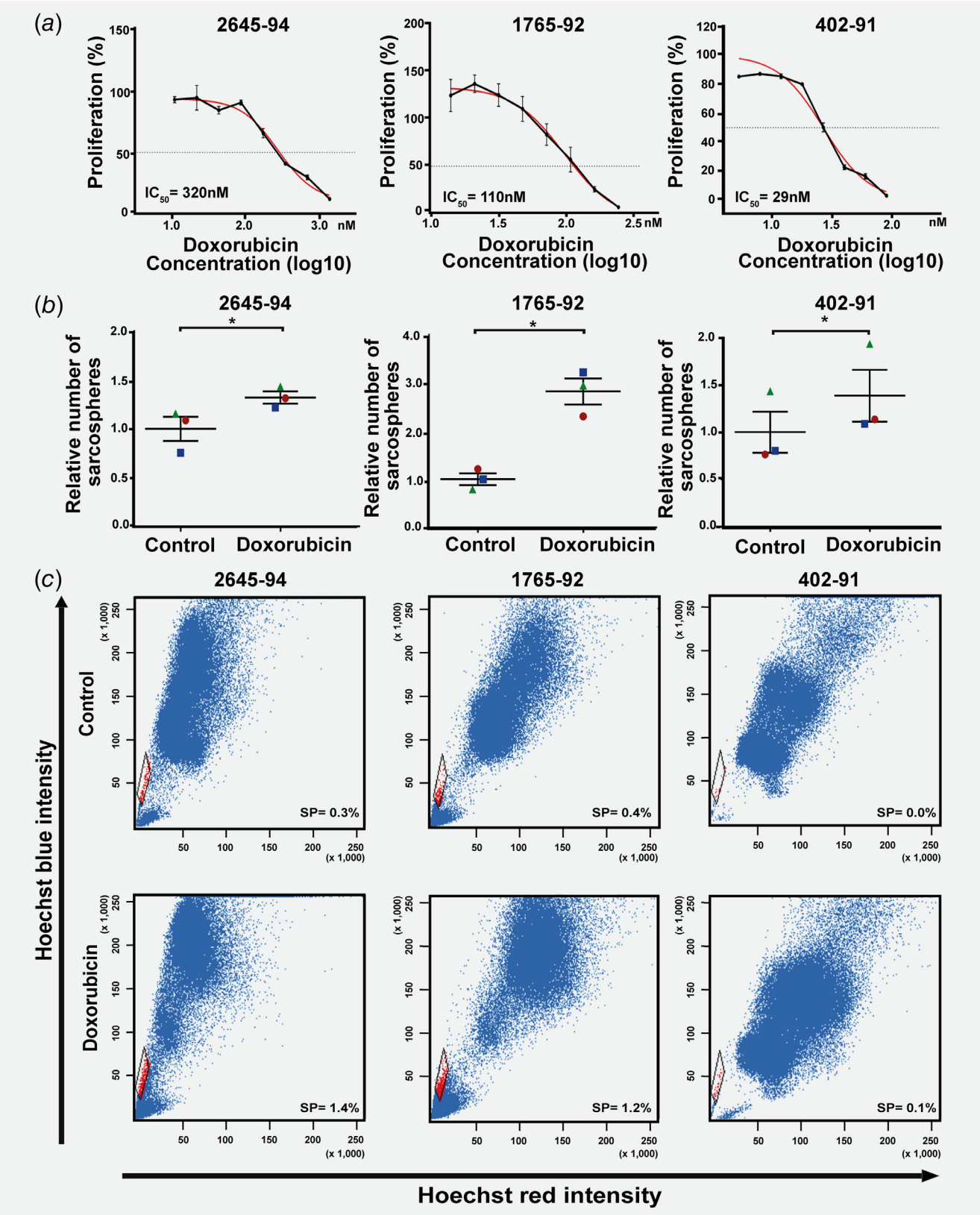

Figure 2. Legend on next page.

10970215, 2019, 2, Downloaded from https://onlinelibrary.wiley.com/doi/10.1002/ijc.32123 by Statens Beredning, Wiley Online Library on [03/06/2023]. See the Terms and Conditions (https://onlinelibrary.wiley.com/terms-and-conditions) on Wiley Online Library for rules of use; OA articles are governed by the applicable Creative Commons License

Table 1. Single-cell gene expression

	MLS 2645-94 (n = 55)			MLS 1765-92 (n = 52)			MLS 402-91 (n = 56)		
Gene name	Pos. cells (%)	Mean	SD	Pos. cells (%)	Mean	SD	Pos. cells (%)	Mean	SD
GAPDH	100	0.0	0.9	98	−0.2	2.3	98	−0.4	1.7
IL6	15	0.0	2.7	12	−0.4	1.9	20	0.5	3.3
LIF	2	0.0	0.3	4	0.0	0.3	11	0.2	0.7
IL6ST (GP130)	100	0.0	1.3	96	−0.7	1.8	93	−1.2	1.6
IL6R	71	0.0	1.6	98	0.4	1.0	70	−0.2	1.4
LIFR	62	0.0	4.0	87	1.3	3.1	77	1.2	3.6
JAK1	95	0.0	3.3	94	0.0	3.0	89	−1.2	3.6
JAK2	49	0.0	5.6	52	0.8	5.7	38	−0.9	5.2
TYK2	78	0.0	6.0	83	−0.1	5.5	77	−0.8	6.1
STAT1	96	0.0	2.6	96	0.3	3.5	95	−0.2	3.1
STAT2	80	0.0	6.2	67	−1.2	6.8	84	1.1	5.8
STAT3	78	0.0	5.2	90	2.5	4.2	95	1.8	3.3
STAT4	0	0.0	0.0	0	0.0	0.0	0	0.0	0.0
STAT5A	80	0.0	2.7	54	−1.4	2.1	79	−0.8	1.7
STAT5B	75	0.0	1.6	83	0.4	1.6	61	−0.5	1.7
STAT6	85	0.0	4.2	37	−6.6	4.4	75	−2.4	4.6
PIAS1	76	0.0	4.9	63	−1.7	5.2	55	−2.7	5.3
PIAS2	40	0.0	2.8	46	−0.1	2.5	64	0.9	2.6
PIAS3	80	0.0	4.8	77	−1.3	4.8	73	−1.2	5.1
PIAS4	80	0.0	2.2	83	−0.1	2.1	75	−0.5	2.1
SOCS1	2	0.0	1.9	2	−0.2	0.7	5	−0.2	0.2
SOCS2	27	0.0	3.0	79	2.9	3.0	52	1.8	3.7
SOCS3	73	0.0	4.7	60	−2.2	4.3	66	−1.5	3.7
SOCS4	64	0.0	5.2	67	−0.3	4.6	48	−1.5	5.3
SOCS5	60	0.0	3.5	71	2.7	4.4	45	−0.6	3.6

Abbreviations: n, number of analysed cells; Pos. cells, percentage of cells expressing each gene; Mean, mean expression of each gene.
The mean expression of each gene was arbitrarily set to a value of one in MLS 2645-94. All expression values are shown in log2-scale, SD: standard deviation.

receptors result in JAK activation, which is followed by *STAT* phosphorylation (Fig. 3*a*).[12] To characterize which canonical JAK–STAT genes that are expressed in MLS, we performed single-cell gene expression profiling. The *JAK* (*JAK1, JAK2* and *TYK2*) and *STAT* (*STAT1-6*) family genes were analyzed together with their inhibitors *PIAS1-4* and *SOCS1-5* genes. In addition, specific cytokines (*IL6* and *LIF*) and cytokine receptors (*IL6R*, *IL6ST* and *LIFR*. *IL6ST* is also known as *GP130*) as well as a housekeeping gene (*GAPDH*) were analyzed. Expression data of each gene displayed only minor differences between the cell lines, both regarding the number of positive cells and their expression levels (Table 1). The largest differences were observed for *SOCS2* and *STAT6*. *SOCS2* was expressed in most cells and to highest degree in MLS 1765-92 followed by MLS 402-91 and MLS 2645-94, while *STAT6* was expressed in most cells and to highest degree in MLS 2645-94 followed by MLS 402-92 and MLS 1765-92. The cytokines *IL6* and *LIF* were expressed in <20% of the cells. The cytokine receptors *IL6R* and *LIFR* were expressed in >50% of the cells and *GP130* was expressed in almost all cells. *JAK1* was

Figure 2. The effects of doxorubicin treatment in MLS. (*a*) Doxorubicin IC_{50} analysis in MLS 2645-94, 1765-92 and 402-91. Dose–response curve after 48 h doxorubicin treatment was generated using Alamar Blue assay. The dashed gray horizontal line indicates 50% relative proliferation. IC_{50} was obtained by applying a symmetrical sigmoidal curve fit. Mean ± SEM is shown, n = 4. (*b*) Sarcosphere formation capacity of MLS cells treated for 48 h with doxorubicin relative control. The graphs show the relative number of sarcopheres formed in control (DMSO) and doxorubicin-treated samples 3 days after cell seeding in non-adherent sphere formation assay. Three independent experiments (green, red and blue) were performed, where each experiment consisted of the average number of spheres formed from three technical replicates. Mean ± SEM is shown, paired student *t*-test $*p < 0.05$. (*c*) Effect of doxorubicin on side population (SP) cells using Hoechst dye staining. The top panel represents control (DMSO) cells, while the bottom panel represents cells treated with doxorubicin for 48 h. The SP cells (red) are gated and their fraction is compared to the total viable cell population. Note that doxorubicin arrests cells in the G2 cell cycle phase. The MLS 402-91 control is identical to the control in Figure 1b, since both experiments were analyzed at the same time. [Color figure can be viewed at wileyonlinelibrary.com]

10970215, 2019, 2, Downloaded from https://onlinelibrary.wiley.com/doi/10.1002/ijc.32123 by Statens Beredning, Wiley Online Library on [05/02/2023]. See the Terms and Conditions (https://onlinelibrary.wiley.com/terms-and-conditions) on Wiley Online Library for rules of use; OA articles are governed by the applicable Creative Commons License

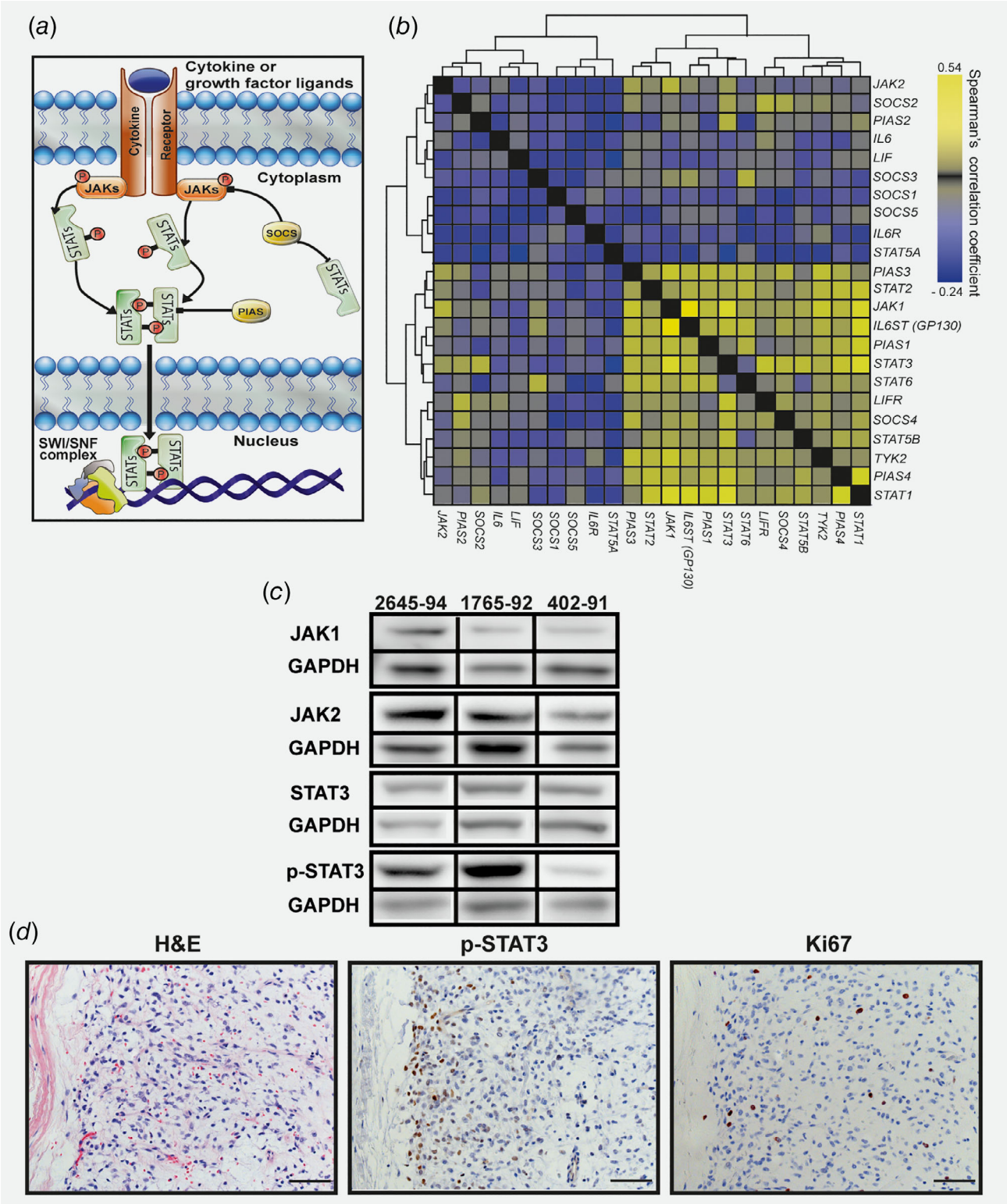

Figure 3. Properties of JAK–STAT signalling in MLS. (*a*) Schematic overview of canonical JAK–STAT signalling. (*b*) Heat-map visualization of pair-wise gene correlations using Spearman's correlation coefficient. (*c*) Western blot analysis of JAK1, JAK2, STAT3 and phospho-STAT3 (p-STAT3) in MLS 2645-94, 1765-92 and 402-91. GAPDH was used as an internal protein loading control. All samples for respective antibody were analysed on the same western blot (Supporting Information Fig. S7). Blot data are cut and reorganized for visualization purposes. (*d*) Immunohistochemical staining of phospo-STAT3 and Ki67 in MLS tumour tissue. Brown staining shows reactivity with the specific antibody. Cells expressing phospho-STAT3 are concentrated at the periphery of a tumour lobule, whereas Ki67-positive cells are scattered throughout the tumour. Scale bar is 0.1 mm. [Color figure can be viewed at wileyonlinelibrary.com]

10970215, 2019, 2, Downloaded from https://onlinelibrary.wiley.com/doi/10.1002/ijc.32123 by Statens Beredning, Wiley Online Library on [03/06/2023]. See the Terms and Conditions (https://onlinelibrary.wiley.com/terms-and-conditions) on Wiley Online Library for rules of use; OA articles are governed by the applicable Creative Commons License

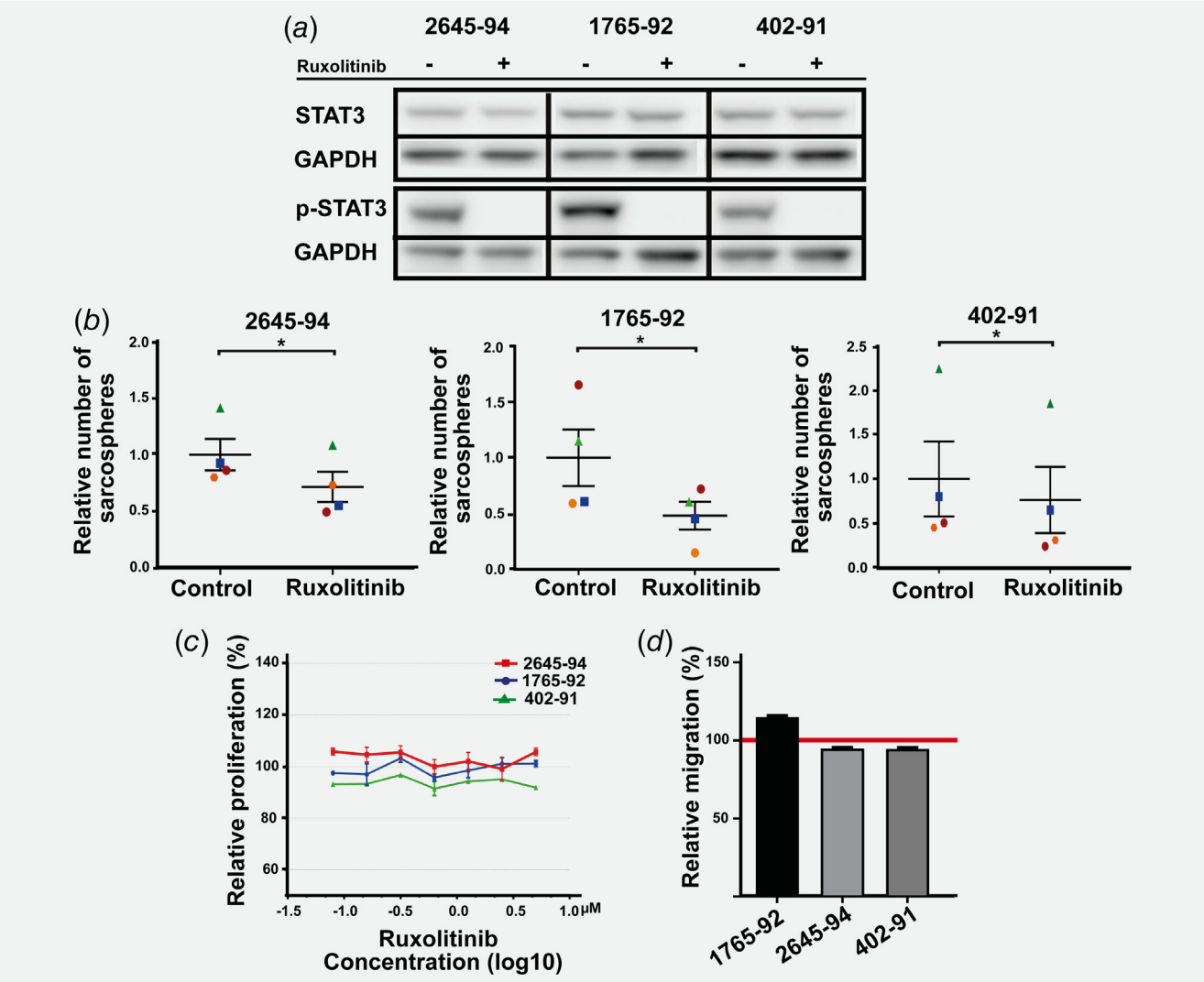

Figure 4. Ruxolitinib inhibits JAK–STAT signalling in MLS. (*a*) Ruxolitinib inhibition of JAK1/2. Western blot analysis of STAT3 and phospho-STAT3 in MLS 2645-94, 1765-92 and 402-91 cells after 24 h ruxolitinib treatment compared to untreated control (DMSO) cells. GAPDH was used as an internal protein loading control. All samples for respective antibody were analysed on the same western blot (Supporting Information Fig. S8). Blot data are cut and reorganized for visualization purposes. (*b*) Sarcosphere formation capacity relative control of MLS cells treated 24 h with ruxolitinib. The graphs show the relative number of sarcospheres formed in control (DMSO) and ruxolitinib-treated samples 3 days after cell seeding in non-adherent sphere-formation assay. Four independent experiments (green, red, orange and blue) were performed, where each experiment consisted of the average number of spheres formed from three technical replicates. Mean ± SEM is shown, paired student *t*-test $*p < 0.05$. (*c*) Effect of ruxolitinib on cell proliferation. Dose response curve of ruxolitinib were generated using the Alamar Blue assay after 48 h treatment. Mean ± SEM is shown, n = 4. (*d*) Effect of ruxolitinib on cell migration. Cell migration was measured using a scratch assay, where the relative migration ratio between control (DMSO) and ruxolitinib-treated cells was calculated. The red line at 100% indicates where ruxolitinib-treated and untreated control cells display identical migration capacity. Mean ± SEM is shown, n = 3. [Color figure can be viewed at wileyonlinelibrary.com]

expressed in 93% of the cells, while *JAK2* and *TYK2* were expressed in 46 and 79% of the cells, respectively. All *STAT* genes, except *STAT4*, were expressed in >50% of the cells in all MLS cell lines. Supporting Information Figure S2 illustrates that all three MLS cell lines display overlapping gene expression profiles. Heat-map clustering of pair-wise gene correlations showed that several (*JAK1*; *TYK2*; *LIFR*; *IL6ST*; *STAT1-3*, *5B* and *6*; *PIAS1*, *3* and *4*, and *SOCS4*) JAK–STAT genes were co-regulated, indicating possible common regulatory elements (Fig. 3*b* and Supporting Information Table S2).[25] Trend principal component analysis of these co-regulated genes shows that all three MLS cell lines contain subpopulation of cells that express low levels of *JAK–STAT* genes, while other subpopulations expressed them at high levels (Supporting Information material: Movie clip).

Signalling pathway, such as JAK–STAT, activity is mainly regulated at protein phosphorylation level. Supporting Information Figure S3 shows the relative phosphorylation level of selected

10970215, 2019, 2, Downloaded from https://onlinelibrary.wiley.com/doi/10.1002/ijc.32123 by Statens Beredning, Wiley Online Library on [05/02/2023]. See the Terms and Conditions (https://onlinelibrary.wiley.com/terms-and-conditions) on Wiley Online Library for rules of use; OA articles are governed by the applicable Creative Commons License

kinases and that all tested STATs (Figs. 2, 3, 5A, 5B and 6) were phosphorylated in the three MLS cell lines. In addition, we confirmed the expression of JAK1, JAK2 and STAT3 proteins using western blot analysis, where MLS 2645-94 and 1765-92 displayed highest levels of phospho-STAT3 (Fig. 3*c*). Immunohistochemical staining of phospho-STAT3 and Ki67 was performed on tumours from nine patients operated for MLS that had not been subjected to neoadjuvant treatment (Fig. 3*d* and Supporting Information Fig. S4). Neoplastic cells with nuclear expression of phospho-STAT3 were present in all cases, although in varying proportions and intensity. The phospho-STAT3 positive cells constituted a minor subpopulation and were mainly

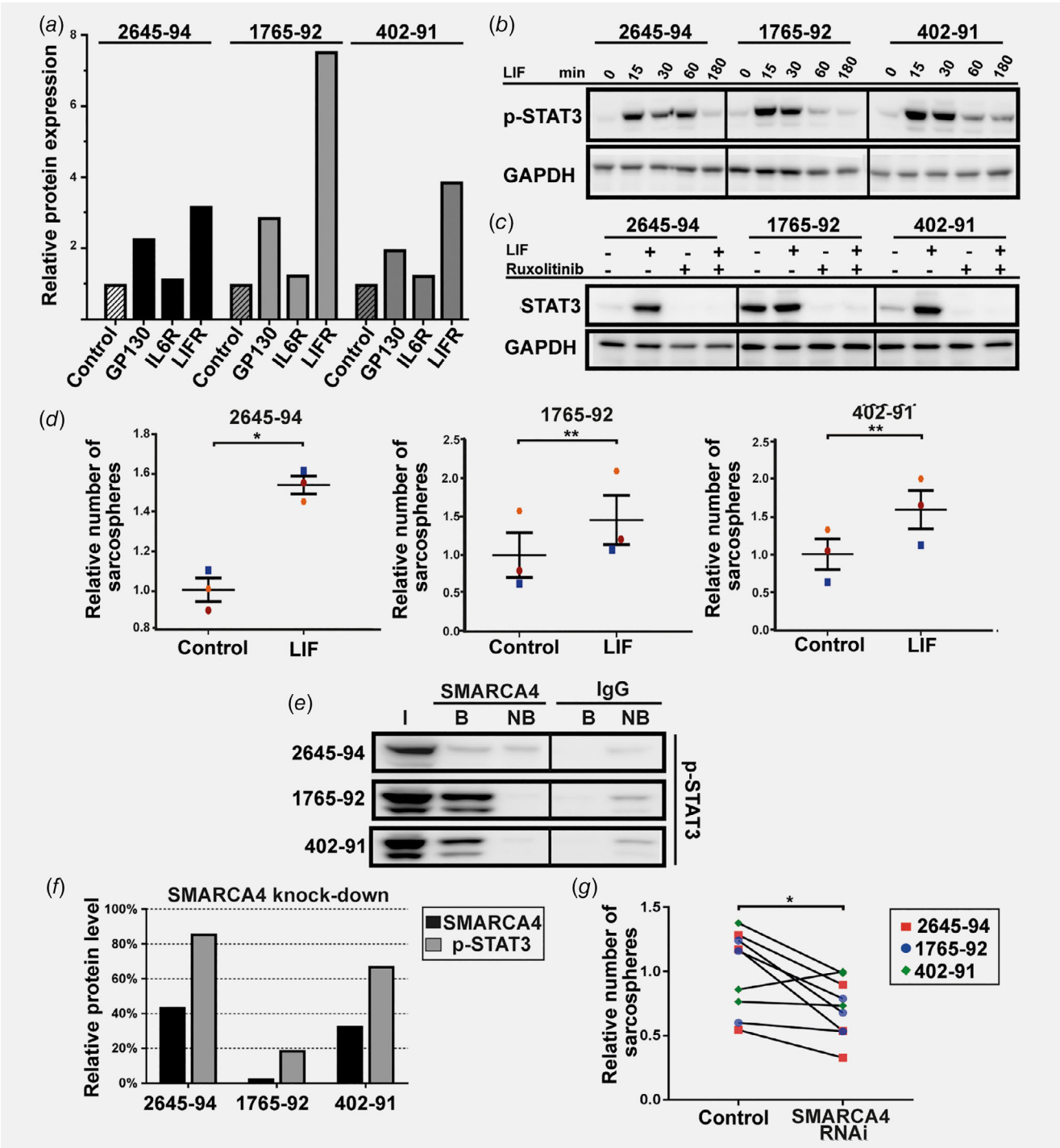

Figure 5. Legend on next page.

Molecular Cancer Biology

10970215, 2019, 2, Downloaded from https://onlinelibrary.wiley.com/doi/10.1002/ijc.32123 by Statens Beredning, Wiley Online Library on [03/06/2023]. See the Terms and Conditions (https://onlinelibrary.wiley.com/terms-and-conditions) on Wiley Online Library for rules of use; OA articles are governed by the applicable Creative Commons License

located in the periphery of tumour lobules beneath a thin fibrous capsule. The staining ranged from scattered individual cells with weak nuclear positivity to contiguous subcapsular clusters of neoplastic cells with strong nuclear reactivity. Some positivity was occasionally noticed in lipoblasts or more mature tumoural adipocytes (Supporting Information Fig. S4). The same pattern of phosho-STAT3 expression was observed in specimens with conventional MLS histology as well as in tumours with a round cell liposarcoma component (data not shown). The fraction of Ki67-positivity was low to moderate with scattered Ki67-positive neoplastic cells present throughout the tumours, without accumulation of positive cells in the peripheral parts of tumour lobules. These data reveal another dimension of tumour cell heterogeneity in MLS with subpopulations with and without activated JAK–STAT signalling.

To examine whether JAK–STAT signalling affects the number of cells forming sarcospheres, we inhibited JAK1/2 with ruxolitinib.[26] Ruxolitinib treatment completely blocked STAT3 phosphorylation in MLS without affecting STAT3 expression levels (Fig. 4*a*) and cells exhibited a 28, 52 and 24% reduction in sarcosphere formation capacity in MLS 2645-94, 1765-92 and 402-91, respectively (Fig. 4*b*). In contrast, JAK1/2 inhibition displayed no effects on either cell proliferation (Fig. 4*c*) or cell migration (Fig. 4*d*). Altogether, these data suggest that JAK–STAT signalling regulated the number of CSCs, but not the number of proliferating cells.

LIF induces CSC properties through JAK–STAT and SWI/SNF signalling

The JAK–STAT pathway can be activated by IL6-type cytokines through dimerization of receptors, including GP130, IL6 and LIF receptors.[27] Using flow cytometry, we observed high expression of LIFR, intermediate expression of GP130, and no or minor expression of IL6R in MLS cell lines (Fig. 5*a* and Supporting Information Fig. S5). These data suggest that LIF is a potential JAK–STAT signalling ligand in MLS. Hence, we treated MLS cells with LIF and demonstrated a rapid increase of phospho-STAT3 levels after 15–30 min stimulation and a decline after 1 h (Fig. 5*b*). The cellular LIF response is in agreement with other reports.[28,29] Furthermore, LIF phosphorylated STAT3 through JAK1/2, since the effect of LIF was completely inhibited by ruxolinitib (Fig. 5*c*). Next, we showed that LIF-treated cells generated 46–58% more sarcospheres than control cells in the three MLS cell lines, indicating that JAK1/2 and STAT3 signalling positively regulate this CSC feature (Fig. 5*d*).

Next, we studied potential downstream protein targets of STAT3. It has been shown that phosphorylated STAT3 acts through interaction with the SWI/SNF complex in mouse embryonic stem cells.[30] To determine if the same mechanism is occurring in MLS, we performed immunoprecipitation with a SMARCA4 antibody (also known as BRG1), a core member of the SWI/SNF complex. Figure 5*e* shows that phosphorylated STAT3 was bound to SMARCA4. Capture of SMARCA4 is shown in Supporting Information Figure S6. To confirm that the observed interaction was important for JAK–STAT signalling we performed knocked-down of SMARCA4 using RNAi. Figure 5*f* shows that phospo-STAT3 was downregulated when the expression of SMARCA4 was decreased. Knock-down of SMARCA4 also resulted in an average 28% reduction in sarcosphere formation capacity (Fig. 5*g*).

JAK–STAT inhibition reduces the number of chemotherapy-resistant cells with CSC properties

To determine if JAK–STAT signalling could affect chemotherapy resistance, we tested the effects of ruxolitinib in combination with doxorubicin using non-adherent sphere formation assay. Figure 6*a* shows that ruxolitinib reduced the number of doxorubicin-enriched sarcospheres. Furthermore, western blot

Figure 5. LIF acts through JAK–STAT and SWI/SNF signalling in MLS. (*a*) Relative protein expression level of IL6R, LIFR and GP130 in MLS 2645-94, 1765-92 and 402-91 cells determined by flow cytometry. Details are shown in Supporting Information Figure S5. (*b*) Western blot analysis of phospho-STAT3 (p-STAT3) expression at different time points after LIF stimuli in MLS cells. GAPDH was used as an internal protein loading control. All samples for respective antibody were analysed on the same western blot (Supporting Information Fig. S9). Blot data are cut and reorganised for visualization purposes. (*c*) Western blot analysis of phospho-STAT3 (p-STAT3) in MLS cells after 24 h treatment with LIF, ruxolitinib or LIF and ruxolitinib in combination. GAPDH was used as an internal protein loading control. All samples for respective antibody were analysed on the same western blot (Supporting Information Fig. S10). Blot data are cut and reorganized for visualization purposes. (*d*) Sarcosphere formation capacity relative control of MLS cells treated 24 h with LIF. The graphs show the relative number of sarcospheres formed in control (1% FBS) and LIF-treated samples 3 days after cell seeding in a non-adherent sphere formation assay. Three independent experiments (orange, red and blue) were performed, where each experiment consisted of the average number of spheres formed from three technical replicates. Mean ± SEM is shown, paired student *t*-test $*p < 0.05$ $**p < 0.01$. (*e*) Co-immunoprecipitation of SMARCA4. Western blot analysis of phosphorylated STAT3 co-immunoprecipitated with nuclear extracted SMARCA4 or IgG. B represents bound phosphorylated STAT3 to SMARCA4 or IgG, and NB represents non-bound phosphorylated STAT3, I represents input material. Corresponding western blots for SMARCA4 are shown in Supporting Information Figure S6. (*f*) SMARCA4 and phospo-STAT3 downregulation after SMARCA4 knock-down using RNAi. The protein expression (in percentage) after knock-down related to control is shown. Each protein expression was normalized against GAPDH expression before comparison. Corresponding western blots are shown in Supporting Information Figure S11. (*g*) Sarcosphere formation capacity of SMARCA4 knock-downed MLS cells. The graph shows the relative number of sarcospheres formed in control and SMARCA4 knock-downed samples 3 days after cell seeding in non-adherent sphere-formation assay. Three independent experiments were performed for each MLS cell line, where each experiment consisted of the average number of spheres formed from three technical replicates. Statistical analysis were performed by Student's paired *t*-test $*p < 0.05$. The reduced sarcosphere formation capacity reached statistical significance only when all three MLS cell lines were analysed together. [Color figure can be viewed at wileyonlinelibrary.com]

10970215, 2019, 2, Downloaded from https://onlinelibrary.wiley.com/doi/10.1002/ijc.32123 by Statens Beredning, Wiley Online Library on [16/02/2023]. See the Terms and Conditions (https://onlinelibrary.wiley.com/terms-and-conditions) on Wiley Online Library for rules of use; OA articles are governed by the applicable Creative Commons License

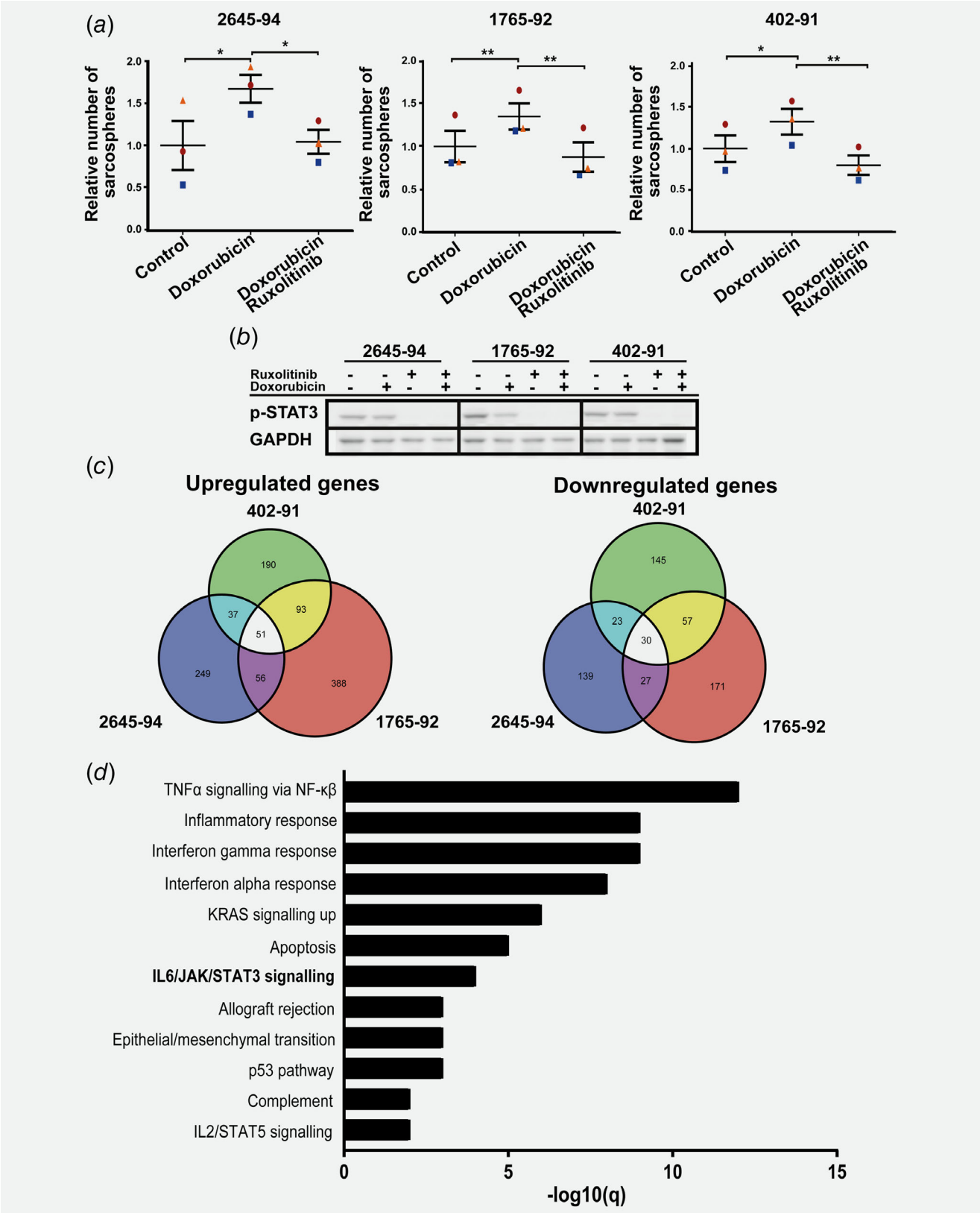

Figure 6. Legend on next page.

Molecular Cancer Biology

10970215, 2019, 2, Downloaded from https://onlinelibrary.wiley.com/doi/10.1002/ijc.32123 by Statens Beredning, Wiley Online Library on [03/06/2023]. See the Terms and Conditions (https://onlinelibrary.wiley.com/terms-and-conditions) on Wiley Online Library for rules of use; OA articles are governed by the applicable Creative Commons License

analysis showed that ruxolitinib completely inhibited phosphorylation of STAT3 also in presence of doxorubicin (Fig. 6*b*).

As JAK–STAT inhibition failed to deplete all sarcospheres we attempted to identify other chemotherapy resistance signalling pathways, by global gene expression profiling comparing doxorubicin-treated cells with control cells. Figure 6*c* shows that 51 genes were at least two-fold upregulated and 30 genes at least two-fold downregulated in all MLS cell lines. For complete gene lists see Supporting Information Table S3. ABC transporter genes were among the upregulated genes. Molecular signature analysis on upregulated genes confirmed JAK–STAT signalling, but also included other pathways and processes such as TNFα signalling *via* NF-κβ, inflammatory response, interferon gamma/alpha response and KRAS signalling (Fig. 6*d*).

Discussion

Doxorubicin and trabectedin are both successfully applied to treat MLS, but not all patients are responding,[31–33] indicating a problem with chemotherapy-resistant cells. Several reports suggest that many cancer forms harbor small distinct subpopulations of tumour cells with stem cell characteristics that are resistant to chemotherapy and responsible for tumour relapse.[11,34] In this study, we showed that MLS cell lines contain subpopulations of cells that can form sarcospheres in a non-adherent sphere formation assay, efflux Hoechst dye and are resistant to the chemotherapy agent doxorubicin. MLS 2645-94 contained most cells with CSC features, followed by MLS 1765-92 and 402-91. The number of cells with CSC properties estimated by non-adherent sphere formation assay and SP analysis correlated between the cell lines, where MLS 2645-94 generated most sarcospheres and contained most SP cells. This cell line was also the most resistant to doxorubicin treatment. The SP analysis and the doxorubicin resistance results are related, since doxorubicin has been shown to be effluxed by ABC transporters.[35] The number of cells with CSC characteristics varied between the non-adherent condition assay and the SP analysis, where the number of formed sarcospheres were 15 and 27 times higher compared to the gated SP cells in MLS 1765-92 and 2645-94, respectively. In MLS 402-91, the number of SP cells was too low to allow any reliable comparison. Our data showed that SP cells were enriched among the cells that formed sarcospheres, but most sarcosphere-forming cells could not efflux the Hoechst dye. SP and non-adherent sphere formation analyses display two different properties related to CSCs. However, these cellular functions are not unique features of all CSC subpopulations[36] and may be shared by other cell types.[19,37] Previous studies have also shown that non-adherent sphere forming assays usually overestimate the number of stem cells by an order of magnitude,[38] indicating that the number of sarcosphere-forming cells in our study only in part reflects the number of true CSCs. Tumour take experiments in mice could reveal further information about the absolute CSC frequency in the tested MLS cell lines.

JAK–STAT signalling is important in tumour initiation,[39] tumour development, and CSC maintenance in several tumour entities, such as gliobastoma,[40] lung,[41] and colon cancer.[42] Our single-cell data showed that individual cultured MLS cells expressed different amounts of canonical JAK–STAT transcripts. JAK1, JAK2 and STATs were also confirmed to be expressed at the protein level. In resection specimens, phospo-STAT3 expression was limited to a subset of cells. Collectively, these data suggest that MLS cells generally have the capacity to use the JAK–STAT pathway, but only a distinct subpopulation displays active JAK–STAT signalling. Today, no well-characterized CSC markers exist for MLS, limiting our possibilities to link specific stemness markers with JAK–STAT expression. Future, whole transcriptome analysis of CSCs at single-cell level may enable the identification of such markers.[43]

Ruxolitinib inhibition of JAK1/2 caused phospo-STAT3 downregulation and decreased the number of formed sarcospheres. Among the MLS cell lines, 1765-92 displayed the highest expression of phospho-STAT3 under normal growth conditions and these cells also showed the largest decrease in sarcosphere formation capacity when treated with ruxolitinib, indicating that the level of phospho-STAT3 correlates with the number of cells with CSC properties. In addition, phosphorylated STAT3 interacted with SMARCA4, a core component of the SWI/SNF complex. Our experiment do not permit conclusions about which specific protein in SWI/SNF that physically interacts with phospo-STAT3, but our knock-down experiment shows that SMARCA4 is key player in JAK–STAT mediated signalling.

Figure 6. Targeting cancer stem cell like cells and proliferating cells as a strategy to treat MLS. (*a*) Sarcosphere formation capacity relative control of MLS 2645-94, 1765-92 and 402-91 cells when treated 48 h with doxorubicin and ruxolitinib in combination. The graphs show the relative number of sarcospheres formed in control (DMSO), doxorubicin- and doxorubicin/ruxolitinib-treated samples 3 days after cell seeding in non-adherent sphere formation assay. Three independent experiments (orange, red and blue) were performed, where each experiment consisted of the average number of spheres formed from three technical replicates. Mean ± SEM is shown, paired student *t*-test $*p < 0.05$ $**p < 0.01$. (*b*) Phospho-STAT3 expression. Western blot analysis of phospho-STAT3 (p-STAT3) in MLS cells after 48 h treatment with doxorubicin, ruxolitinib or doxorubicin and ruxolitinib in combination. GAPDH was used as an internal protein loading control. All samples for respective antibody were analysed on the same western blot (Supporting Information Fig. S12). Blot data are cut and reorganized for visualization purposes. (*c*) Microarray analysis. Venn diagrams showing the number of genes, after filtering, with a two-fold upregulation or downregulation in doxorubicin-treated MLS cells. (*d*) Bar chart showing, out of the 51 genes upregulated in all three cell lines, significantly enriched (FDR *q*-value <0.05) gene sets among the Hallmark gene sets from the Molecular Signatures Database. [Color figure can be viewed at wileyonlinelibrary.com]

10970215, 2019, 2, Downloaded from https://onlinelibrary.wiley.com/doi/10.1002/ijc.32123 by Statens Beredning, Wiley Online Library on [05/05/2023]. See the Terms and Conditions (https://onlinelibrary.wiley.com/terms-and-conditions) on Wiley Online Library for rules of use; OA articles are governed by the applicable Creative Commons License

The SWI/SNF complex acts as a chromatin remodeling system known to regulate stem cell properties through STAT3,[30,44] further supporting the hypothesis that JAK–STAT signalling controls CSC features in MLS. We also showed that the upstream JAK–STAT receptors GP130 and LIFR were expressed in MLS cell lines. LIF, a LIFR ligand and growth factor known to maintain stem cells,[45] elevated the number of sarcospheres through JAK1/2 signalling. A possible source of LIF is the MLS cells themselves, but our single-cell data showed that only few MLS cells expressed LIF transcripts. Another potential source of LIF is secretion from stromal cells, which was reported for other tumour entities.[46,47] Other cytokines and their receptors may also be important activators of JAK–STAT signalling in MLS.

Our data showed that the doxorubicin-resistant cells belonged to the subpopulation of cells with CSC characteristics. A reduction of CSC-like cells could thus be expected to improve the effect of this drug. Indeed, our results confirmed that inhibition of JAK–STAT signalling decreased the number of cells with CSC properties that resisted doxorubicin treatment. By combining doxorubicin and ruxolitinib, we targeted both proliferating cells and cells with CSC properties, resulting in improved drug effects. Still, some doxorubicin-resistant cells with CSC properties lacking active JAK–STAT signalling remained. This observation was expected, since ruxolitinib-treatment of control MLS cells failed to eliminate all cells with the capacity to form sarcospheres. Our microarray data support JAK–STAT signalling as being a key process in doxorubicin resistance. However, doxorubicin also regulated TNFα and KRAS signalling, indicating their involvement in chemotherapy resistance. In addition, other cellular processes, including RET,[48] IGF[49] and SRC[50] signalling, are also active in MLS and are therefore potential regulators of CSC properties in MLS.

In conclusion, our data show that MLS cell lines contain subpopulations of cells with CSC properties defined by sphere-forming capacity, ability to efflux Hoechst dye and resist chemotherapy. JAK–STAT signalling is active in MLS and regulates the size of the CSC-like subpopulation. JAK1/2 inhibition enforced the effects of doxorubicin by reducing the number of both proliferating and CSC-like cells. Future *in vivo* studies are required to confirm the clinical use of JAK–STAT inhibition, but our results suggest that JAK–STAT inhibition combined with chemotherapy or similar drug combinations could improve treatment of MLS patients.

Conflict of interest

AS declares stock ownership in TATAA Biocenter.

Acknowledgements

We thank Susann Busch, Paul Fitzpatrick and Christoffer Vannas, Sahlgrenska Cancer Center, Department of Pathology and Genetics, Institute of Biomedicine, Sahlgrenska Academy at University of Gothenburg, Sweden for valuable discussions; Shahin De Lara, Department of Clinical Pathology and Genetics, Sahlgrenska University Hospital, Sweden for technical assistance with immunohistochemistry and Vladimir Benes and Jelena Pistolic, Genomics Core Facility, EMBL, Heidelberg, Germany for microarray analysis.

Author contributions

S.D. and A.S. conceived the study. S.D., M.L., B.F., K.B., M.N. and A.M. performed the experiments. S.D., E.J., A.F., H.F., G.L., P.Å. and A.S. analysed data. S.D., E.J., P.Å. and A.S. drafted the manuscript and all authors read and approved the final manuscript.

References

1. Andersson MK, Ståhlberg A, Arvidsson Y, et al. The multifunctional FUS, EWS and TAF15 proto-oncoproteins show cell type-specific expression patterns and involvement in cell spreading and stress response. *BMC Cell Biol* 2008;9:37.
2. Blechingberg J, Luo Y, Bolund L, et al. Gene expression responses to FUS, EWS, and TAF15 reduction and stress granule sequestration analyses identifies FET-protein non-redundant functions. *PLoS One* 2012;7:e46251.
3. Riggi N, Cironi L, Suva ML, et al. Sarcomas: genetics, signalling, and cellular origins. Part 1: the fellowship of TET. *J Pathol* 2007;213:4–20.
4. Åman P. Fusion oncogenes of sarcomas. In: Rowley DJ, Le Beau MM, Rabbitts TH, eds *Chromosomal translocations and genome rearrangements in cancer*. New York: Springer International Publishing Switzerland Springer, 2015. 321–54.
5. Fletcher CDM, Unni KK, Mertens F. *Tumors of soft tissue and bone*. Lyon, France: IARC Press, 2000.
6. Ståhlberg A, Kåbjörn Gustafsson C, Engtröm K, et al. Normal and functional TP53 in genetically stable Myxoid/round cell Liposarcoma. *PLoS One* 2014;9:e113110.
7. Engstrom K, Willen H, Kabjorn-Gustafsson C, et al. The myxoid/round cell liposarcoma fusion oncogene FUS-DDIT3 and the normal DDIT3 induce a liposarcoma phenotype in transfected human fibrosarcoma cells. *Am J Pathol* 2006;168: 1642–53.
8. Dolatabadi S, Candia J, Akrap N, et al. Cell cycle and cell size dependent gene expression reveals distinct subpopulations at single-cell level. *Front Genet* 2017;8:1.
9. Kåbjörn-Gustafsson C, Ståhlberg A, Danielsson A, et al. Cell senescence in myxoid/round cell liposarcoma. *Sarcoma* 2014;2014:1–7.
10. Kabjorn Gustafsson C, Ståhlberg A, Engtrom K, et al. Cell senescence in myxoid/round cell liposarcoma. *Sarcoma* 2014;2014:208786.
11. Dean M, Fojo T, Bates S. Tumour stem cells and drug resistance. *Nat Rev Cancer* 2005;5:275–84.
12. Buchert M, Burns CJ, Ernst M. Targeting JAK kinase in solid tumors: emerging opportunities and challenges. *Oncogene* 2016;35:939–51.
13. Thomas SJ, Snowden JA, Zeidler MP, et al. The role of JAK/STAT signalling in the pathogenesis, prognosis and treatment of solid tumours. *Br J Cancer* 2015;113:365–71.
14. Åman P, Ron D, Mandahl N, et al. Rearrangement of the transcription factor gene CHOP in myxoid liposarcomas with t(12;16)(q13; p11). *Genes Chromosomes Cancer* 1992;5: 278–85.
15. Harrison H, Farnie G, Howell SJ, et al. Regulation of breast cancer stem cell activity by signaling through the Notch4 receptor. *Cancer Res* 2010;70: 709–18.
16. Goodell MA. Stem Cell Identification and Sorting Using the Hoechst 33342 Side Population (SP). *Curr Protoc Cytom* 2005;33:1–11.
17. Goodell MA, Brose K, Paradis G, et al. Isolation and functional properties of murine hematopoietic stem cells that are replicating in vivo. *J Exp Med* 1996;183:1797–806.
18. Ståhlberg A, Rusnakova V, Forootan A, et al. RT-qPCR work-flow for single-cell data analysis. *Methods (San Diego, CA)* 2013;59:80–8.
19. Tirino V, Desiderio V, Paino F, et al. Cancer stem cells in solid tumors: an overview and new approaches for their isolation and characterization. *FASEB J* 2013;27:13–24.
20. Zhou B-BS, Zhang H, Damelin M, et al. Tumour-initiating cells: challenges and opportunities for

10970215, 2019, 2, Downloaded from https://onlinelibrary.wiley.com/doi/10.1002/ijc.32123 by Statens Beredning, Wiley Online Library on [03/06/2023]. See the Terms and Conditions (https://onlinelibrary.wiley.com/terms-and-conditions) on Wiley Online Library for rules of use; OA articles are governed by the applicable Creative Commons License

anticancer drug discovery. *Nat Rev Drug Discov* 2009;8:806–23.
21. Katz D, Boonsirikamchai P, Choi H, et al. Efficacy of first-line doxorubicin and ifosfamide in myxoid liposarcoma. *Clin Sarcoma Res* 2012;2:2.
22. Robey RW, To KK, Polgar O, et al. ABCG2: a perspective. *Adv Drug Deliv Rev* 2009;61:3–13.
23. Wan S, Zhao E, Kryczek I, et al. Tumor-associated macrophages produce interleukin 6 and signal via STAT3 to promote expansion of human hepatocellular carcinoma stem cells. *Gastroenterology* 2014;147:1393–404.
24. Villalva C, Martin-Lanneree S, Cortes U, et al. STAT3 is essential for the maintenance of neurosphere-initiating tumor cells in patients with glioblastomas: a potential for targeted therapy? *Int J Cancer* 2011;128:826–38.
25. Volfson D, Marciniak J, Blake WJ, et al. Origins of extrinsic variability in eukaryotic gene expression. *Nature* 2006;439:861–4.
26. Zhou T, Georgeon S, Moser R, et al. Specificity and mechanism-of-action of the JAK2 tyrosine kinase inhibitors ruxolitinib and SAR302503 (TG101348). *Leukemia* 2014;28:404–7.
27. Heinrich PC, Behrmann I, Haan S, et al. Principles of interleukin (IL)-6-type cytokine signalling and its regulation. *Biochem J* 2003;374:1–20.
28. Onishi K, Zandstra PW. LIF signaling in stem cells and development. *Development* 2015;142:2230–6.
29. Matsuda T, Nakamura T, Nakao K, et al. STAT3 activation is sufficient to maintain an undifferentiated state of mouse embryonic stem cells. *EMBO J* 1999;18:4261–9.
30. Ho L, Miller EL, Ronan JL, et al. esBAF facilitates pluripotency by conditioning the genome for LIF/STAT3 signalling and by regulating polycomb function. *Nat Cell Biol* 2011;13:903–13.
31. Gronchi A, Bui B, Bonvalot S, et al. Phase II clinical trial of neoadjuvant trabectedin in patients with advanced localized myxoid liposarcoma. *Ann Oncol* 2012;23:771–6.
32. Patel SR, Andrew Burgess M, Plager C, et al. Myxoid liposarcoma. Experience with chemotherapy. *Cancer* 1994;74:1265–9.
33. Grosso F, Jones RL, Demetri GD, et al. Efficacy of trabectedin (ecteinascidin-743) in advanced pretreated myxoid liposarcomas: a retrospective study. *Lancet Oncol* 2007;8:595–602.
34. Vidal SJ, Rodriguez-Bravo V, Galsky M, et al. Targeting cancer stem cells to suppress acquired chemotherapy resistance. *Oncogene* 2014;33:4451–63.
35. Calcagno AM, Fostel JM, To KKW, et al. Single-step doxorubicin-selected cancer cells overexpress the ABCG2 drug transporter through epigenetic changes. *Br J Cancer* 2008;98:1515–24.
36. Golebiewska A, Brons NH, Bjerkvig R, et al. Critical appraisal of the side population assay in stem cell and cancer stem cell research. *Cell Stem Cell* 2011;8:136–47.
37. Pastrana E, Silva-Vargas V, Doetsch F. Eyes wide open: a critical review of sphere-formation as an assay for stem cells. *Cell Stem Cell* 2011;8:486–98.
38. Reynolds BA, Rietze RL. Neural stem cells and neurospheres—re-evaluating the relationship. *Nat Methods* 2005;2:333–6.
39. Chen K, Huang YH, Chen JL. Understanding and targeting cancer stem cells: therapeutic implications and challenges. *Acta Pharmacol Sin* 2013;34:732–40.
40. Ganguly D, Pfeffer L. Dysregulated signaling pathways in glioblastoma cancer stem-like cells: potential targets for therapeutic intervention. *MOJ Cell Sci Rep* 2016;3:00051.
41. Dutta P, Sabri N, Li J, et al. Role of STAT3 in lung cancer. *Jak-Stat* 2014;3:e999503.
42. Matsui WH. Cancer stem cell signaling pathways. *Medicine* 2016;95:S8–S19.
43. Karlsson J, Kroneis T, Jonasson E, et al. Transcriptomic characterization of the human cell cycle in individual unsynchronized cells. *J Mol Biol* 2017;429:3909–24.
44. Ho L, Ronan JL, Wu J, et al. An embryonic stem cell chromatin remodeling complex, esBAF, is essential for embryonic stem cell self-renewal and pluripotency. *Proc Natl Acad Sci U S A* 2009;106:5181–6.
45. Chen C-YY, Lee DS, Yan Y-TT, et al. Bcl3 bridges LIF-STAT3 to Oct4 signaling in the maintenance of Naïve Pluripotency. *Stem Cells (Dayton, Ohio)* 2015;33:3468–80.
46. Crichton MB, Nichols JE, Zhao Y, et al. Expression of transcripts of interleukin-6 and related cytokines by human breast tumors, breast cancer cells, and adipose stromal cells. *Mol Cell Endocrinol* 1996;118:215–20.
47. Royuela M, Ricote M, Parsons MS, et al. Immunohistochemical analysis of the IL-6 family of cytokines and their receptors in benign, hyperplasic, and malignant human prostate. *J Pathol* 2004; 202:41–9.
48. Safavi S, Jarnum S, Vannas C, et al. HSP90 inhibition blocks ERBB3 and RET phosphorylation in myxoid/round cell liposarcoma and causes massive cell death in vitro and in vivo. *Oncotarget* 2016;7:433–45.
49. Trautmann M, Menzel J, Bertling C, et al. FUS-DDIT3 fusion protein-driven IGF-IR signaling is a therapeutic target in myxoid liposarcoma. *Clin Cancer Res* 2017;23:6227–38.
50. Sievers E, Trautmann M, Kindler D, et al. SRC inhibition represents a potential therapeutic strategy in liposarcoma. *Int J Cancer* 2015;137: 2578–88.

10970215, 2019, 2, Downloaded from https://onlinelibrary.wiley.com/doi/10.1002/ijc.32123 by Statens Beredning, Wiley Online Library on [05/12/2023]. See the Terms and Conditions (https://onlinelibrary.wiley.com/terms-and-conditions) on Wiley Online Library for rules of use; OA articles are governed by the applicable Creative Commons License